H-Plane-Scanning Multibeam Leaky-Wave Antenna for Wide-Angular-Range AoA Estimation at mm-wave”

Julien Sarrazin, Guido Valerio

H-Plane-Scanning Multibeam Leaky-Wave Antenna for Wide-Angular-Range AoA Estimation at mm-wave

Julien Sarrazin*, Guido Valerio*,
*Sorbonne Université, CNRS, Laboratoire de Génie Electrique et Electronique de Paris, 75252, Paris, France
Université Paris-Saclay, CentraleSupélec, CNRS, Laboratoire de Génie Electrique et Electronique de Paris, 91192, Gif-sur-Yvette, France, julien.sarrazin@sorbonne-universite.fr

***Abstract*—A fully-metallic periodic leaky-wave antenna well-suited for angle-of-arrival estimation with a reduced frequency bandwidth is presented. The design is based on a leaky rectangular waveguide loaded with corrugations and periodically modulated by longitudinal slots, which produces a frequency beam scanning in the H-plane. By exploiting multiple visible spatial harmonics, multiple beams are radiated for each frequency. This enables the antenna main beam to scan the 180°-angular range with a bandwidth of only 3.7% at 27 GHz. Simulations show that using a frequency-domain MUSIC approach, it is possible to estimate angles-of-arrival of several incoming sources without ambiguity.**

***Index Terms*—Leaky-wave antennas, periodic structure, corrugated rectangular waveguide, angle-of-arrival estimation, MUSIC.**

I. Introduction

Millimeter-wave (mm-wave) communications typically requires highly directional antennas to achieve sufficient link-budgets, raising the issue of beam alignment between the two ends of the wireless communication. This is possible if an angles-of-arrival (AoA) estimate is available. Leaky-wave antennas (LWA) represent a cost-effective solution to estimate AoA at mm-wave frequencies, due to their natural beam-scanning behaviour with frequency [1]. However, the applicability of this approach in mobile communication applications is limited since LWA commonly need a large operational bandwidth in order to scan a large field of view (FoV).

This issue has been tackled in the literature with different approaches. At mm-wave, the LWA scanning velocity has been improved by loading the leaky guiding structure with a dense metasurface [2] or by adding an extra dispersive lens [3]. However, the required bandwidth to scan a large FoV remains larger than typical frequency channels used in telecommunications. The works in [4], [5] exploit several multiport LWAs while [6] use reconfigurable LWAs. These approaches achieves AoA estimation over a large FoV at the expense of cost and/or complexity.

An alternative approach is to use periodic LWAs that radiate multiple beams at each frequency [7]. This is achieved by designing the LWA to support multiple fast spatial harmonics that contribute to the far-field radiation. In doing so, the FoV is divided by the number of beams per frequency, which in turns greatly reduces the required bandwidth. It was shown in [7], [8] that a subspace algorithm such as MUSIC can distinguish the AoAs of incoming sources among the multiple beams. A preliminary antenna design of multibeam LWA is presented in [8] and achieves an E-plane scanning. Being implemented in a dielectric-filled waveguide, it is therefore suffering from dielectric losses.

This paper presents a fully-metallic LWA able to scan in the H-plane in the 28 GHz band. The unit-cell of the periodic LWA is described in Section II together with its dispersion analysis. The design of the LWA as well as its performance are discussed in Section III. Section IV performs AoA estimation using the proposed multibeam LWA and Section V concludes this paper.

II. Unit-cell analysis

The proposed periodic antenna is based on the unit-cell shown in Fig. 1 (geometrical parameters are given in the caption). It consists in a longitudinal slot etched in a rectangular waveguide in order to achieve an H-plane frequency scanning of the LWA beams. To increase frequency scanning velocity, the lower plate of the rectangular waveguide is filled with corrugations. This increases the effective index without using any lossy dielectric. The spatial period p is large and is chosen in such a way to generate several fast spatial harmonics. The unit-cell is simulated with Ansys HFSS and the S parameters are used to calculate the complex propagation constant of the periodic structure as described in [9]. The phase constant $\beta^n = \beta^0 + 2\pi n/p$, with β^0 the phase constant of the uniformly corrugated waveguide, is shown in Fig. 2. The solid lines represent the visible spatial harmonics of a wave propagating towards +z axis while the dashed ones represent the wave propagating towards -z axis. In the 26.5-27.5 GHz frequency band, 5 spatial harmonics are visible and will therefore be responsible for the radiation of up to 5 beams towards the directions approximately given by $\theta^n = \sin^{-1}(\beta^n/k_0)$, where k_0 is the free space wavenumber. Three examples are given in Fig. 2, where the radiation direction is computed from the phase constant. Over this 1-GHz bandwidth, it is observed that the β^n values span almost continuously the $[-k_0 : k_0]$ interval. Consequently, an angular scanning from $\theta = -90°$ to $\theta = +90°$ can be theoretically achieved by designing a

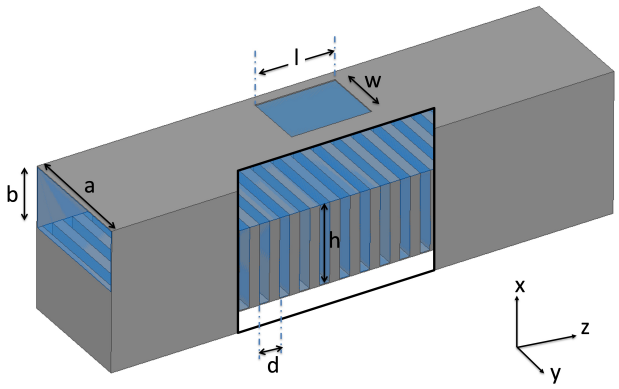

Fig. 1: Unit-cell of length $p = 25$ mm. Slot center is offset by 1 mm from the waveguide center longitudinal axis ($a = 6$ mm, $b = 3$ mm, $w = 3$ mm, $l = 4$ mm, $d = 1$ mm, $h = 4$ mm).

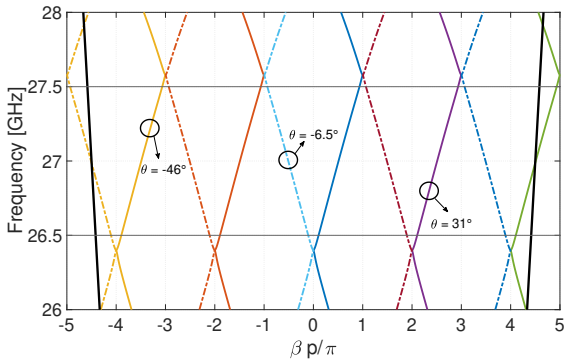

Fig. 2: Phase constants of the periodic structure. Lines of light $\beta = \pm k_0$ (*black lines*).

LWA based on this unit-cell. Multibeam operation effectively divides the FoV into smaller angular sectors, each of them being covered by the frequency scanning of one of the multiple beams. This approach allows for a complete FoV coverage with a reduced frequency bandwidth. With no corrugation inside the rectangular waveguide, more spatial harmonics are required to achieve a continuous spanning over the $[-k_0 : k_0]$ range within the 1-GHz bandwidth. Generating more visible spatial harmonics requires a larger spatial period which in turns raises design issues as discussed in [8].

III. LWA DESIGN

The proposed LWA design based on the unit cell presented in the previous section is shown in Fig. 3. It is composed of 10 unit cells. At the input ports, a non-corrugated 3-mm-long input section ends on a 15-mm-long tapering section where the corrugations depth linearly increases. The overall LWA length is 265 mm. The simulated S-parameters are shown in Fig. 4 with and without considering the ohmic losses. In the lossless case, the transmission coefficient in the 26.5-27.5 GHz range is relatively constant at about -10 dB, which indicates that most of the input power has been radiated (about

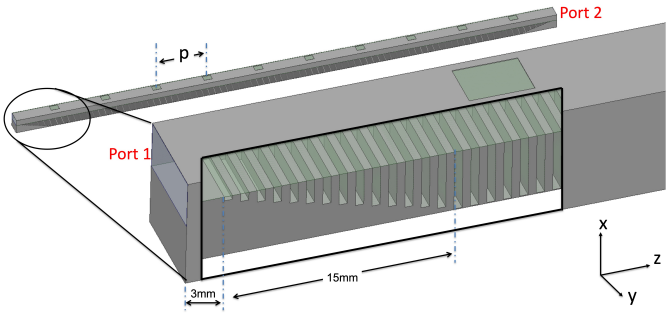

Fig. 3: Leaky wave antenna design ($p = 25$ mm): the inset shows the tapering section.

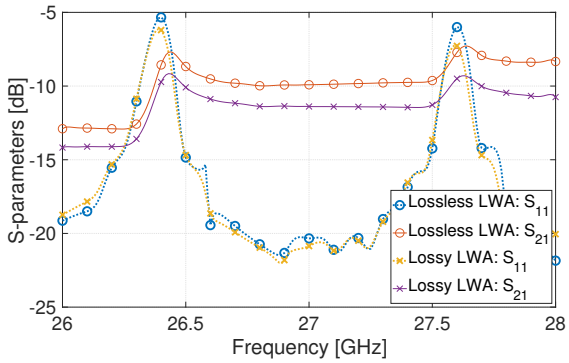

Fig. 4: S-parameters of the LWA without and with metallic losses (copper is used for the lossy case).

90% radiation efficiency). In this same band, the reflection coefficient remains below -15 dB. By taking into account losses, the transmission coefficient drops by about 1.4 dB in the band of interest, thereby lowering the radiation efficiency.

The simulated realized gain is shown in Fig. 5 for the H-plane copolarization (XZ plane) with an excitation on port 1 for the solid lines and on port 2 for the dashed ones. Depending on the frequency, up to 5 beams are radiated whose directions scan with frequency. The number of beams and their directions are in good agreement with the dispersion analysis in Fig. 2. This is visualized by the three beams pointing in the directions computed in Fig. 2 on the relevant harmonics. An almost continuous beam scanning is observed over the angular range when considering excitation by both LWA ports. At the edge of the frequency band, there is a drop in the gain due to the vicinity of the stop-bands, as can be observed in Fig. 2. This behaviour could be mitigated with techniques such as in [10], [11]. The maximum realized gain is 13.8 dB. The multiple beams do not exhibit a constant amplitude among them, with a decrease as the beams steer towards end-fire, as expected according to the electric field orientation that is tangential to the waveguide upper plate. The spatial harmonics $n = -1$, $n = -2$, and $n = 0$, are, respectively, the most excited ones. Overall, the gain variation over the 180°-angular range is about 15 dB. With a maximum accepted gain variation of 10 dB (resp. 6 dB), the angular coverage is $\pm 63°$ (resp. $\pm 50°$).

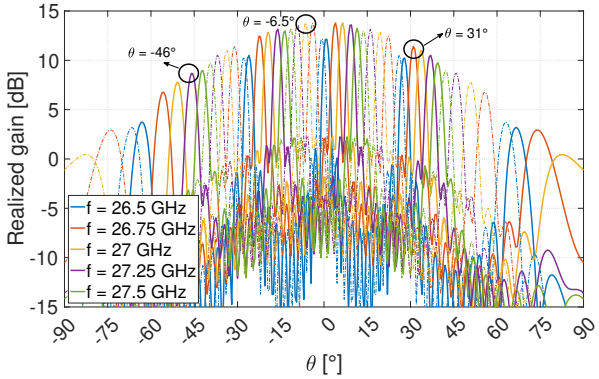

Fig. 5: Realized gain of the 10-unit-cell LWA. Solid lines: port 1 excitation. Dotted lines: port 2 excitation.

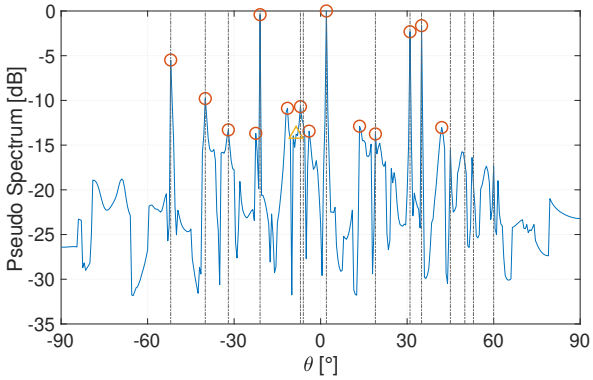

Fig. 6: MUSIC pseudo spectrum obtained from received signal at port 1.

IV. AoA estimation

A. MUSIC system model

To perform an AoA estimation of D plane waves impinging on the LWA, the MUSIC algorithm is used on the signals received by both the LWA ports. The D sources are considered to be modulated using a multicarrier scheme. By assuming that all subcarriers carry the same data $\mathbf{s}$, the following frequency-domain system model is obtained:

$$\begin{bmatrix} x_1[k] \\ \vdots \\ x_M[k] \end{bmatrix} = \begin{bmatrix} a_1(\theta_1) & \dots & a_1(\theta_D) \\ \vdots & \ddots & \vdots \\ a_M(\theta_1) & \dots & a_M(\theta_D) \end{bmatrix} \cdot \begin{bmatrix} s_1[k] \\ \vdots \\ s_D[k] \end{bmatrix} + \begin{bmatrix} z_1[k] \\ \vdots \\ z_M[k] \end{bmatrix} \tag{1}$$

with $\mathbf{x} \in \mathbb{C}^{M\times 1}$, the data vector received by either the LWA port 1 or 2, $\mathbf{A} \in \mathbb{C}^{M\times D}$, the LWA response matrix of the corresponding port, $\mathbf{s} \in \mathbb{C}^{D\times 1}$, the source vector, $\mathbf{z} \in \mathbb{C}^{M\times 1}$, a complex Additive White Gaussian Noise (AWGN) vector with uncorrelated components, and $k = 1, \dots, K$ is the kth snapshot among K. M is the number of frequency samples, i.e., number of subcarriers, as opposed to the number of single antenna elements in a typical linear-array-based MUSIC scheme. Each column of $\mathbf{A}$ represents the LWA response to an incoming plane wave of AoA $\theta_{i=1,\dots,D}$ and is obtained by HFSS simulations.

The MUSIC pseudo spectrum is calculated on each port as:

$$P(\theta) = \frac{\mathbf{a}(\theta)^{\mathbf{H}}\mathbf{a}(\theta)}{\mathbf{a}(\theta)\{\mathbf{E_N}\mathbf{E_N^H}\}\mathbf{a}(\theta)} \tag{2}$$

where $\mathbf{E_N}$ is the matrix that contains the noise eigenvectors of the covariance matrix, estimated as $\mathbf{R} = \frac{1}{K}\mathbf{x}\mathbf{x}^{\mathbf{H}}$.

B. Results and performance

Simulated MUSIC pseudo spectrums are shown in Fig. 6, Fig. 7, and Fig. 8, from signals received at port 1, at port 2, and at both ports, respectively. The pseudo spectrum making use of the signals received at both ports is obtained by the Hadamard product of the single-port-calculated pseudo spectrums. The simulation is performed with $D = 14$ uncorrelated incoming sources of AoA $\theta = \{-52°, -40°, -32°, -21°, -7°, -6°, 2°, 19°, 31°, 35°, 45°, 50°, 53°, 60°\}$, an SNR of 15 dB, $K = 200$ snapshots, and $M = 144$ frequency samples. The true AoA are indicated by vertical black dashed lines. The orange circles correspond to the D strongest peaks in the spectrum and the triangle corresponds to the $(D+1)th$ strongest peak, i.e., the strongest spurious peak which does not correspond to an actual source.

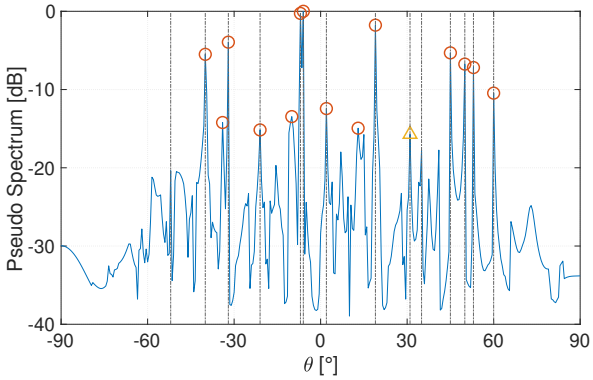

Fig. 7: MUSIC pseudo spectrum obtained from received signal at port 2.

It can be observed that using only port 1 or 2, the sources whose AoA fall in the angular regions where the LWA main beam does not scan are not well detected. As an example, AoAs with $\theta = 45°$, $50°$, $53°$, and $60°$ are missed while processing the signal received at port 1 and AoAs with $\theta = -52°$ $31°$, and $35°$ are missed while processing the signal received at port 2. However, using both ports allows for a perfect retrieval of the AoAs as seen in Fig. 6. The ratio between the lowest true AoA peak and the strongest spurious peaks is 3 dB in this example. This ratio increases as the SNR increases and/or as the number of snapshots K increases (not shown here).

V. Conclusion

A leaky-wave antenna (LWA) exhibiting an original multi-beam operation is proposed to overcome scanning range

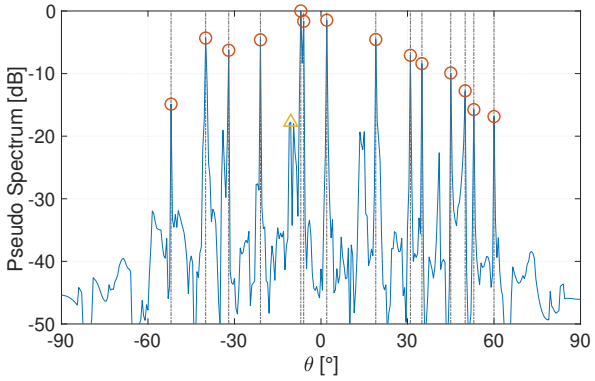

Fig. 8: MUSIC pseudo spectrum obtained from received signals at port 1 and 2.

limitations typically encountered in LWA in limited frequency bands. A rectangular waveguide as a leaky structure is chosen due to its low-loss behavior making it suitable for mm-wave applications. To increase frequency beam scanning velocity with frequency, corrugations are implemented in the lower plate of the waveguide, which increases the effective refractive index without the need for filling the waveguide with a lossy dielectric. The structure is geometrically modulated by periodically etching longitudinal slots to produce a beam scanning in the H-plane. The spatial period is purposely chosen to obtain 5 spatial harmonics in the visible domain in the 26.5-27.5 GHz band, leading to up to 5 radiated beams for each single frequency. The $180°$-angular range is therefore divided into 5 smaller angular sectors, which greatly reduced the required bandwidth to cover the whole angular range. Consequently, by processing the signals received by the two ends of the LWA, the $180°$-angular range is covered with a bandwidth as small as 3.7%. The proposed approach is assessed with simulations with a frequency-domain MUSIC algorithm which enables estimating AoA of a large number of sources without ambiguity among the multiple beams radiated by each particular frequency. This concept could be used to perform real-time AoA estimation operating over frequency bandwidths compatible with typical wireless communication channels.

Acknowledgment

This work was supported by the ANR BeSensiCom project, grant ANR-22-CE25-0002-01 of the French Agence Nationale de la Recherche, and carried out in the framework of COST Action CA20120 INTERACT.

References

[1] A. A. Oliner and D. R. Jackson, "Leaky-wave antennas," in *Antenna Engineering Handbook*, J. Volakis, Ed. New York: McGraw-Hill, 2007, ch. 11.

[2] Q. Zhang, J. Sarrazin, M. Casaletti, G. Valerio, P. De Doncker, A. Benlarbi-Delai, "Enhanced Scanning Range Design for Leaky-Wave Antenna (LWA) at 60 GHz", 13th European Conference on Antennas and Propagation (EuCAP), Krakow, Poland, 1-5 April 2019

[3] X. Zeng, Q. Chen, O. Zetterstrom, and O. Quevedo-Teruel, "Fully Metallic Glide-Symmetric Leaky-Wave Antenna at K?-Band With Lens-Augmented Scanning," in IEEE Transactions on Antennas and Propagation, vol. 70, no. 8, pp. 7158-7163, Aug. 2022, doi: 10.1109/TAP.2022.3146855.

[4] M. K. Emara, D. J. King, H. V. Nguyen, S. Abielmona, and S. Gupta, "Millimeter-Wave Slot Array Antenna Front-End for Amplitude-Only Direction Finding," in IEEE Trans. on Antennas and Propagation, vol. 68, no. 7, pp. 5365-5374, July 2020, doi: 10.1109/TAP.2020.2979284.

[5] M. Poveda-García, A. Gómez-Alcaraz, D. Cañete-Rebenaque, A. S. Martinez-Sala and J. L. Gómez-Tornero, "RSSI-Based Direction-of-Departure Estimation in Bluetooth Low Energy Using an Array of Frequency-Steered Leaky-Wave Antennas," in IEEE Access, vol. 8, pp. 9380-9394, 2020, doi: 10.1109/ACCESS.2020.2965233.

[6] H. Paaso, et Al., "DoA estimation through modified unitary MUSIC algorithm for CRLH leaky-wave antennas," IEEE PIMRC, London, 2013, pp. 311-315, doi: 10.1109/PIMRC.2013.6666152.

[7] J. Sarrazin, "MUSIC-based Angle-of-Arrival Estimation using Multi-beam Leaky-Wave Antennas," URSI GASS 2021, Rome, Italy, 28 August - 4 September 2021

[8] J. Sarrazin and G. Valerio, "Multibeam Leaky-Wave Antenna for Mm-wave Wide-Angular-Range AoA Estimation," 2022 16th European Conference on Antennas and Propagation (EuCAP), 2022, pp. 1-5, doi: 10.23919/EuCAP53622.2022.9769571.

[9] D. M. Pozar, "Microwave filters," in *Microwave Engineering*. Hoboken, NJ, USA: Wiley, 2011, ch. 8.

[10] D. K. Karmokar, S. -L. Chen, D. Thalakotuna, P. -Y. Qin, T. S. Bird and Y. J. Guo, "Continuous Backward-to-Forward Scanning 1-D Slot-Array Leaky-Wave Antenna With Improved Gain," in IEEE Antennas and Wireless Propagation Letters, vol. 19, no. 1, pp. 89-93, Jan. 2020, doi: 10.1109/LAWP.2019.2953927.

[11] Z. Liu, H. Lu, J. Liu, S. Yang, Y. Liu and X. Lv, "Compact Fully Metallic Millimeter-Wave Waveguide-Fed Periodic Leaky-Wave Antenna Based on Corrugated Parallel-Plate Waveguides," in IEEE Antennas and Wireless Propagation Letters, vol. 19, no. 5, pp. 806-810, May 2020, doi: 10.1109/LAWP.2020.2980993.